

Optical Engineering

OpticalEngineering.SPIEDigitalLibrary.org

Antenna-based microwave absorber for imaging in the frequencies of 1.8, 2.45, and 5.8 GHz

Fatih Ozkan Alkurt
Olcay Altintas
Ahmet Atci
Mehmet Bakir
Emin Unal
Oguzhan Akgol
Kemal Delihacioğlu
Muharrem Karaaslan
Cumali Sabah

SPIE.

Fatih Ozkan Alkurt, Olcay Altintas, Ahmet Atci, Mehmet Bakir, Emin Unal, Oguzhan Akgol, Kemal Delihacioğlu, Muharrem Karaaslan, Cumali Sabah, "Antenna-based microwave absorber for imaging in the frequencies of 1.8, 2.45, and 5.8 GHz," *Opt. Eng.* **57**(11), 113102 (2018), doi: 10.1117/1.OE.57.11.113102.

Antenna-based microwave absorber for imaging in the frequencies of 1.8, 2.45, and 5.8 GHz

Fatih Ozkan Alkurt,^a Olcay Altintas,^a Ahmet Atci,^a Mehmet Bakir,^b Emin Unal,^a Oguzhan Akgol,^a Kemal Delihacioğlu,^c Muharrem Karaaslan,^a and Cumali Sabah^{d,e,*}

^aIskenderun Technical University, Department of Electrical and Electronics Engineering, Iskenderun, Hatay, Turkey

^bBozok University, Faculty of Engineering and Architecture, Department of Computer Engineering, Yozgat, Turkey

^cKilis 7 Aralik University, Department of Electrical and Electronics Engineering, Kilis, Turkey

^dMiddle East Technical University—Northern Cyprus Campus, Department of Electrical and Electronics Engineering, Kalkanli, Guzelyurt, Mersin, Turkey

^eMiddle East Technical University—Northern Cyprus Campus, Kalkanli Technology Valley, Kalkanli, Guzelyurt, Mersin, Turkey

Abstract. We propose a microwave imaging structure with GSM, ISM, Wi-Fi, and WiMAX operating frequencies at 1.80, 2.45, and 5.80 GHz, respectively. The suggested structure is based on a microwave antenna-inspired absorber with cavities in resonator layers. Our study, which is validated using simulation and experimental techniques, deals with the absorption of the incident electromagnetic waves at 1.80, 2.45, and 5.80 GHz for creating the image when radio frequency microwave is employed. The above-mentioned three operating frequencies, by which electromagnetic waves are radiated from three different antennas, are read via digital oscilloscope and finally these voltages are converted to 256 gray-leveled pixel values of each cell. During the experimental testing, simulated and tested values complied with each other. Small differences occurred due to calibration and testing errors. The novelty of this study is having image capability with most commonly used frequency bands by absorbing microwave energy. © 2018 Society of Photo-Optical Instrumentation Engineers (SPIE) [DOI: 10.1117/1.OE.57.11.113102]

Keywords: metamaterials; absorber; antenna; microwave imaging.

Paper 180996 received Jul. 9, 2018; accepted for publication Oct. 31, 2018; published online Nov. 21, 2018.

1 Introduction

Nowadays, applications of wireless communications and power transfers are increasing with the development of technology such as Bluetooth, Wi-Fi, 3G-4G, and WLAN.^{1–5} Also technologies cause electromagnetic (EM) pollution in the area around us.^{6–8} These undesired EM waves can be absorbed using various techniques,^{9–20} which mainly confine incident EM waves between resonators. In addition to this, the incident EM wave confined in the absorber can also be gathered by energy harvesters.^{21–25} To implement perfect absorption, Landy et al.⁹ analyzed, characterized, and fabricated two coupled metamaterial structures to demonstrate operating principle of metamaterial structure at the frequency of 11.50 GHz. The coupled resonators lie in parallel in front and back sides of each cell to confine and absorb incident power. To obtain wideband absorption, Xin et al.¹² developed an absorber with the continuous ground plane and square resonators to absorb and confine microwaves with the frequencies of 32 GHz and bandwidth of nearly 22-GHz. In another study, a dual-band metamaterial-based polarization-independent and tunable microwave absorber is designed and suggested by Yu et al.¹³ In addition, a dual-band metamaterial-based absorber was proposed for WLAN-WiMAX bands especially at 3.50 and 5.80 GHz, respectively.¹⁴ In addition, Bakir et al.¹⁶ suggested a tunable perfect metamaterial absorber using a varactor diode. Karaaslan et al.¹⁹ developed an absorber structure to absorb and harvest incident microwaves for wireless communication bands. Almoreef and Ramahi²¹ designed a metamaterial-based absorber structure that has perfect absorption characteristics

at 3 GHz. Energy harvesting from radiated radio frequency (RF) signals is investigated by Heydari Nasab et al.²³

To harvest incident energy, some processes are needed as a rectification process.^{26–29} In addition, different structures used as rectifier-integrated antennas are called as rectennas.^{30–35} Gao et al.²⁶ proposed a rectifier structure using CMOS technology that can be used in wireless power transfer applications such as 2.40 GHz. In the literature, there are many studies that contain rectification of 2.45 GHz with high efficiencies.^{27–31} Other studies presented rectification at 5.80 GHz, which is in the wireless communication band.^{32,33} Moreover, there are some studies based on an absorber and energy harvester to obtain an image of incident microwaves.^{36–39} Xie et al.³⁶ suggested a 6.30-GHz microwave camera, which is based on metamaterial absorber. Ghasr et al. developed a real-time microwave camera for the frequency of 24 GHz using an array of slot antennas.³⁷ Also they designed a wideband microwave camera to operate in the range of 20 to 30 GHz, which is capable of 3-D images.³⁸

This paper presents an imaging structure that is based on a microwave signal absorber. In the design and simulation parts, finite integration technique (FIT)-based microwave solver is used. The designed microwave absorber structure absorbs incident waves at the frequencies of 1.80, 2.45, and 5.80 GHz, respectively. Under normal incidence, the designed structure has 95.6%, 84.1%, and 89.8% absorption, respectively. The electric field distributions are different at different resonances; therefore, these differences cause voltage difference at resonance frequencies of 1.80, 2.45, and 5.80 GHz, respectively. In the imaging operation, the designed structure is fabricated as a 5 × 6 array and each

*Address all correspondence to: Cumali Sabah, E-mail: sabah@metu.edu.tr

cell is represented by 256 gray levels with voltage differences. The novelty of the study is that the proposed metamaterial absorber experimentally demonstrates strong imaging characteristic specifically at commonly used communication bands of GSM, ISM, Wi-Fi, and WIMAX with absorption ratios of 0.97, 0.95, and 0.93, respectively. These high absorption values have been harvested at each unit cell as a pixel to high imaging contrast. The advantages of the study over the alternatives^{13,14,19,27,36,37} are the compatibilities of the structure to three commonly used communication bands and metamaterial absorber characteristic.

2 Background and Design

Radiated RF and microwave energy can be absorbed and harvested with different techniques as mentioned before. Rectennas and metamaterial structures are often seen in the literature to absorb and harvest incident energies. This study proposes a three-band signal absorber-based image detector. In the design part, FIT based on a commercial microwave simulator (CST Design Environment) is used. The designed unit cell of microwave signal absorber consists of two resonator layers as shown in Fig. 1, yellow layers denote copper resonators. Other than this, the designed unit structure is composed of three layers such as metal back plate, substrate layer, and resonator layer. In the design of the resonator layer and metal back plate, copper is chosen and it has thickness of 0.035 mm and conductivity of 5.8×10^7 S/m. Also FR-4 dielectric is used in the substrate layer with thickness of 1.6 mm, permittivity of 4.3, and loss tangent of 0.025, respectively. Dimension parameters of the designed absorber are obtained using a genetic algorithm tool, which is presented by a simulation program and obtained dimensions are given in Table 1. As shown in Table 1, each unit cell has 38-mm edge length and consists of two resonator layers. Each resonator is inspired from rectangle-shaped ring and gaps in each ring are also rectangle shaped.

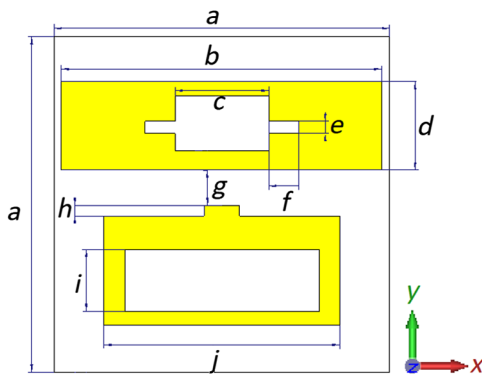


Fig. 1 Front view of designed unit cell structure.

Table 1 Design parameters of designed unit cell structure.

Parameter	a	b	c	d	e	f	g	h	i	j
Value (mm)	38	36.3	10.6	10	1.38	3.4	4	1.2	7	26.72

3 Simulation and Experiment

Simulations are also carried out in FIT-based commercial microwave simulation software and boundaries are adjusted as electric field $E = 0$ in the x-direction, magnetic field $H = 0$ in the y-direction, and open in the z-direction, respectively. This kind of arrangement creates transverse electromagnetic (TEM) mode incident EM wave. Therefore, absorption capability of the proposed structure is investigated under TEM mode microwaves. The power intensity in simulation is 1 Watt and the simulation uses power ratios with respect to this value. The incident power adjusted in the experimental setup is 5 dBm with a maximum power, and the study was carried out with the absorption of this power at the related frequency ranges. Absorption can be calculated by the equation of $A = 1 - T - R$, where A , T , and R refer absorption, transmission, and reflection, respectively. In other words, transmission T and reflection R can be expressed by scattering parameters as $T = |S_{21}|^2$ and $R = |S_{11}|^2$. The proposed absorber contains a copper back plate as mentioned before, which causes minimum transmission, which is nearly zero. The final absorption equation is rearranged as $A = 1 - R = 1 - |S_{11}|^2$.

The designed absorber structure is examined at 1 to 6 GHz TEM mode incident microwaves in a microwave simulator. Obtained absorption characteristics are shown in Fig. 2. Three absorption peaks are observed and absorption peaks occur at 1.80, 2.45, and 5.80 GHz, respectively. As shown in Fig. 2, 1.80, 2.45, and 5.80 GHz have 95.6%, 84.1%, and 89.8% absorptions, respectively. According to absorption characteristics, the proposed structure can be used as EM wave absorber in GSM, ISM, Wi-Fi, and WIMAX frequency bands.

To see the effects of each resonator on the absorption, electric field distributions are obtained from the microwave simulator as shown in Fig. 3. In this numerical analysis, a Floquet port is used for each resonance frequency to obtain electric field distribution. The applied wave is in TEM mode for the Floquet port with a distance adjusted to far-field application. The same results can also be observed for different antenna types located to far-field distance from the structure. Each resonator has different electric field distributions. Under 1.80-GHz incident microwave, electric field distribution is concentrated on the upper resonator as shown in Fig. 3(a). Likewise, under 2.45-GHz incident microwave, electric field distribution is concentrated on the lower resonator as shown in Fig. 3(b) and electric field distribution is

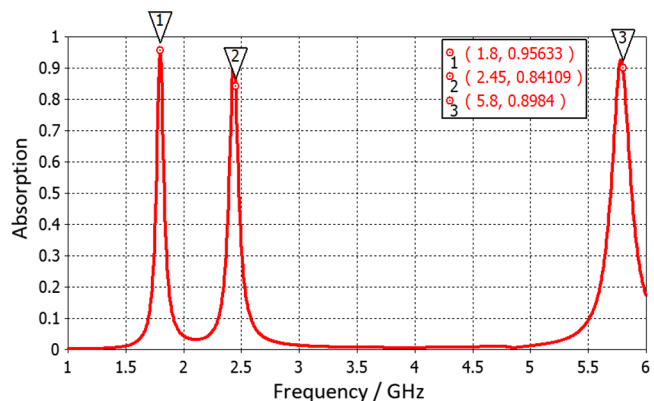


Fig. 2 Absorption characteristics of designed structure.

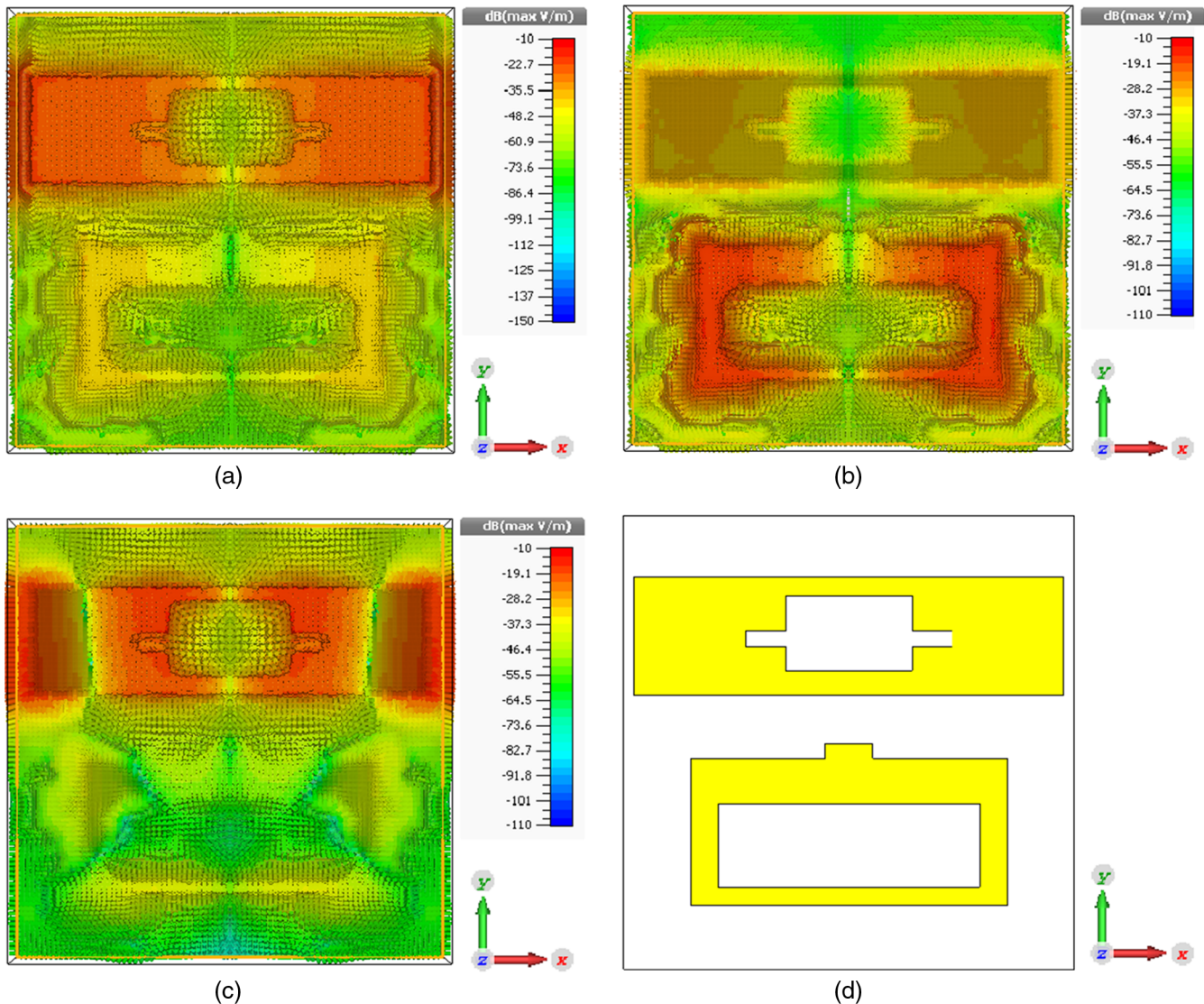


Fig. 3 Electric field distribution at: (a) 1.80 GHz, (b) 2.45 GHz, (c) 5.80 GHz, and (d) front view of designed absorber.

observed with small diffraction on the upper resonator at 5.80 GHz as shown in Fig. 3(c). In addition, the front view of proposed absorber is shown in Fig. 3(d).

The designed three-band absorber is fabricated with 5×6 unit cell array as shown in Fig. 4 using LPKF ProtoMat-E33 Printed Circuit Board (PCB) production machine. A Rohde and Schwarz vector network analyzer and a wideband horn antenna are used to obtain absorption characteristics of the fabricated structure, also given in Fig. 4. Before the absorption measurement, experimental kits are calibrated for impedance matching between the antenna and vector network analyzers according to current state of the art. When the 1- to 6-GHz incident microwaves are applied by wideband horn antenna, reflections are obtained from the vector network analyzer. Distance in the far field can be calculated with respect to the largest antenna dimension using the equation of far-field distance $\geq 2D^2/\lambda$, where D is the largest antenna dimension and λ is the operating wavelength.³⁹ The minimum far-field distance of the largest dimension of the used antenna (8 cm) has been evaluated as 7.68 cm for minimum resonance frequency of 1.8 GHz as shown

in Fig. 4. As mentioned before, absorption can be calculated from scattering parameter S_{11} ; therefore, absorption characteristics of fabricated structure are shown in Fig. 5. Maximum peaks are observed at 1.85, 2.57, and 5.82 GHz and some unwanted noises are seen in the experiment because of laboratory conditions. The resonance frequency shifts in terms of percentage of the central frequencies at 1.8 and 2.45 GHz are 2.7% and 4.1%, respectively. In addition to this, the shift cannot be verified at 5.8 GHz by the same approach due to the inconsistency of bandwidths between measurement and simulation results. In parallel, these unexpected frequency shifts are observed because of fabrication imperfection such as soldering. Moreover, the experimental data have a wider band compared with the simulated ones. This unexpected wider band at 5.80 GHz stems from laboratory conditions such as scatterers around experimental setup, soldering, fabrication imperfection, and noises.

MATS-1000 antenna training system is calibrated and used for operating at the frequency range between 300 MHz and 6 GHz.⁴⁰ The main advantage of using the antenna

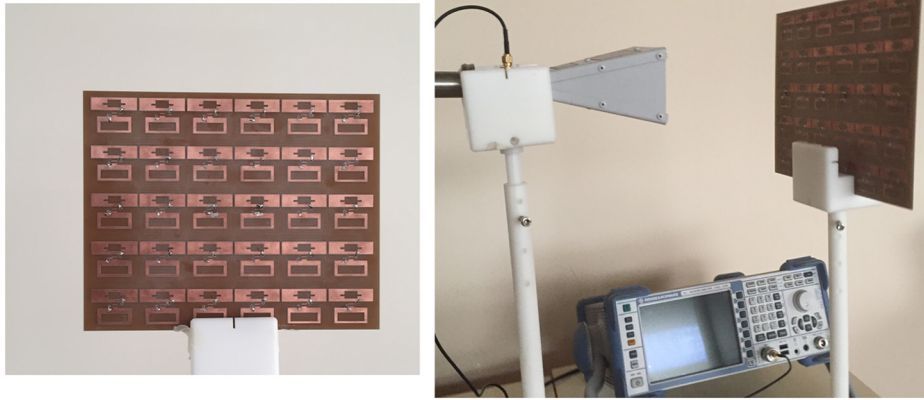


Fig. 4 Fabricated 5×6 array absorber and experimental setup.

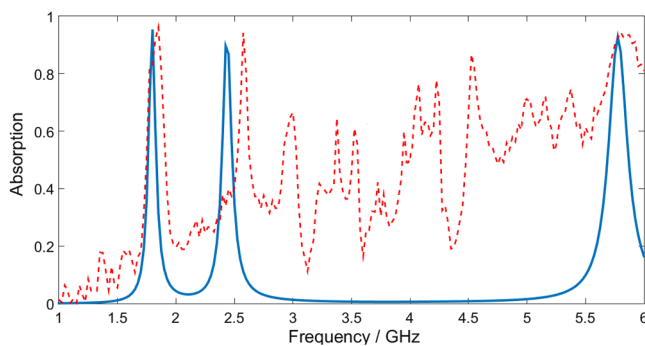


Fig. 5 Absorption characteristics of simulation and experimental measurement.

trainer system is to have maximum 5-dBm incident microwave power. When the incident microwaves are applied from the patch antenna to absorber structure, each resonator has voltage on it as electric field distribution similar to simulation, which is discussed before. Consequently, under incident microwave power, voltage measurement is carried out as shown in Fig. 6. To measure the voltage on each unit cell, small size holes are drilled near the gap of each unit cells. A digital oscilloscope is used to measure voltage difference and the probe's noise sensitivity is decreased nearly zero level to obtain noiseless voltage signal.

Therefore, minimum 6-mV RMS voltage is observed without incident microwave power. Obtained minimum



Fig. 6 Voltage signal measurement via digital oscilloscope probe.

signals are converted to pixel values with 0 to 55 mV scale as shown in Fig. 7. MATLAB is used in the voltage-to-pixel conversion operation. Then 2.57-GHz incident microwaves are applied using 2.45-GHz wideband patch antenna and maximum 53-mV RMS voltage signal is obtained on the resonator layer. Obtained voltages on 5×6 array absorber are converted to pixel values with 0- to 55-mV scale as shown in Fig. 8, whereas each cell absorbs nearly the same amount of incident microwave power. However, obtained images are not fully symmetric as can be seen in Figs. 7 and 8 due to inaccurate placement of the copper block and the fabrication errors such as drilling on each resonator and soldering parts.

To see the image capability of designed absorber structure, a metal plate is located between the patch antenna and absorber as shown in Fig. 9. In theory, a metal reflects or absorbs incident microwaves, and transmission must be zero via the metal layer. To demonstrate microwave signal transfer via the metal plate, the aluminum plate is used to block transmission and the obtained image is shown in Fig. 9. According to the obtained image, transferred power is decreased half of its maximum value against the fact that all the signals will be cut off. So all incident signals cannot be blocked by the aluminum plate due to its dimensions (50 cm \times 50 cm) and side lobes effects, which stem from the edges of aluminum plate. Although larger plate dimensions exactly prevent transmission of incident wave, the 50- \times 50-cm aluminum plate is used due to not have in laboratory equipment. Because the skin depth of the metallic sheet (from 2.6 to 1.05 μm) with a thickness of 0.5 cm at the related frequency range is sufficient to block the incident wave, a single aluminum plate has been used.

The fabricated absorber has good absorption characteristics as explained before, and another experiment is conducted with a 5.80-GHz Yagi-Uda antenna to see image capability of the fabricated structure at 5.80 GHz. Yagi-Uda antennas are directional antennas and located as shown in Fig. 10. Maximum 28-mVRMS voltage is observed under incident microwave power from Yagi-Uda antenna. Image capability is also obtained by MATLAB environment and scaled between 0 and 30 mV as shown in Fig. 10, the directivity of Yagi-Uda antenna is different than patch antenna because it causes the different voltage scales. The similar pixel inaccuracies, which are caused by different transferred power values, are observed in both 2.45 and 5.8 GHz with

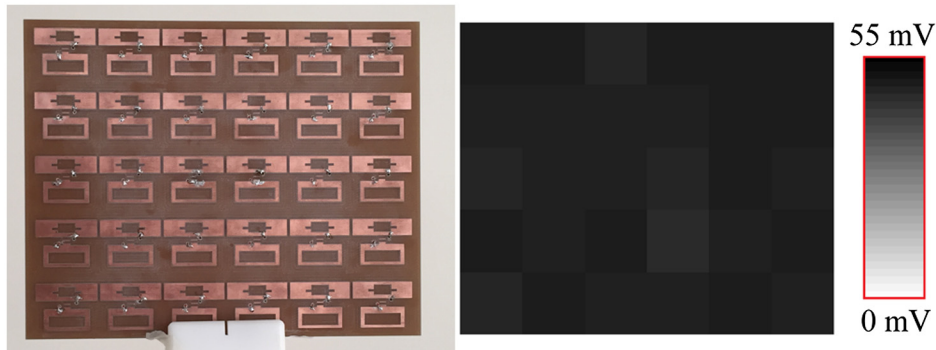


Fig. 7 Image without incident EM signals.



Fig. 8 Image under 2.57-GHz incident EM signals.

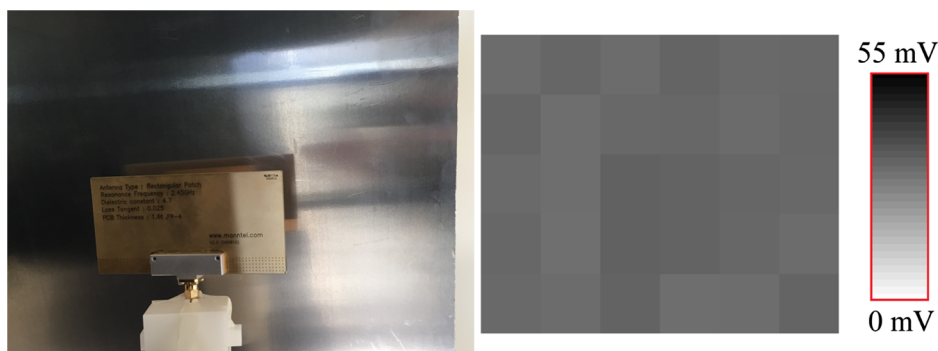


Fig. 9 Image under 2.57-GHz incident EM signals with aluminum plate in front of the absorber.

the patch antenna and Yagi-Uda antenna, respectively. This observed similarity stems from fabrication errors as drilling and soldering. About 5-dBm incident microwave power is transmitted from Mats-1000 antenna training system via professional Yagi-Uda antenna toward the absorber structure. The measured absorption is 93% at 5.82 GHz; therefore, the absorbed power can be evaluated as 4.65 dBm for 5-dBm incident power at 5.82 GHz. Each cell absorbs power at 5.80-GHz incident microwave power, but absorption levels are not the same as shown in Fig. 10. These differences are occurred from laboratory conditions and fabrication imperfections.

Furthermore, a metal plate is located between the Yagi-Uda antenna and absorber structure as shown in Fig. 11.

Measured voltage signals on each resonator layer are reduced to half of its maximum value as obtained in the previous experiment. The aluminum metal plate is not cut-off transmission fully because the metal is not big enough and its width is not too thick. Each unit cell of the metamaterial absorber is a part of the entire structure. In metamaterial applications, behavior of unit cell has similarity with overall structure. In addition to this, the undesired interaction between nearby unit cells cannot be eliminated. Hence, in this study, this interaction is also observed between nearby unit cells as can be seen from Figs. 8 and 10, respectively. This undesired interaction will be avoided in future studies using small microwave band gap surfaces by minimizing surface currents.



Fig. 10 Image under 5.80-GHz incident EM signals.



Fig. 11 Image under 5.80-GHz incident EM signals with aluminum plate in front of the absorber.

4 Conclusions

In this paper, a three-band microwave power absorber-based image detector is proposed for the frequencies of 1.80, 2.45, and 5.80 GHz. First, the proposed structure is designed in a FIT-based microwave simulator and then 5×6 array absorber is fabricated by CNC-based PCB machine. Therefore, the fabricated structure is tested using a vector network analyzer and a horn antenna, and then an absorption characteristic is obtained by experimental measurement. According to the obtained absorption characteristic, resonance frequencies are seen at 1.85, 2.57, and 5.82 GHz and this result shows that there are small frequency shifts in resonance frequencies after fabrication. In addition, image capability of the fabricated absorber is tested under resonance frequencies. Maximum 53-mV RMS voltage signal is obtained at 2.57 GHz and 28-mV RMS voltage signal is observed at 5.82 GHz. In fact, each cell absorbs and induces a voltage signal on its resonator layer, which makes each resonator has antenna behavior. 2.57- and 5.82-GHz microwaves are applied by a patch antenna and a Yagi-Uda antenna, respectively. Moreover, obtained voltage signal on each resonator converted to pixel value to create the image of incident microwave power. Also incident power is blocked by an aluminum plate to see effect of metal plate between antenna absorber layers. To sum up, image capability of a three-band microwave absorber is discussed in this paper. The proposed absorber can be used as a microwave image detector in some applications, e.g., nondestructive imaging, incident microwave tracing, and medical areas.

References

1. J. S. Lee et al., "A comparative study of wireless protocols: Bluetooth, UWB, ZigBee, and Wi-Fi," in *Industrial Electronics Society, 2007 (IECON 2007). 33rd Annual Conference of the IEEE*, pp. 46–51, IEEE (2007).
2. T. Salonidis et al., "Distributed topology construction of Bluetooth wireless personal area networks," *IEEE J. Sel. Areas Commun.* **23**(3), 633–643 (2005).
3. X. Li et al., "The future of mobile wireless communication networks," in *Int. Conf. on Communication Software and Networks (ICCSN 2009)*, pp. 554–557, IEEE (2009).
4. H. Inamura et al., *TCP Over Second (2.5 G) and Third (3G) Generation Wireless Networks (No. RFC 3481)* (2003).
5. A. H. Khan et al., "4G as a next generation wireless network," in *Int. Conf. on Future Computer and Communication (ICFCC 2009)*, pp. 334–338, IEEE (2009).
6. A. Ahlbom and M. Feychting, "Electromagnetic radiation: environmental pollution and health," *Br. Med. Bull.* **68**(1), 157–165 (2003).
7. S. Cucurachi et al., "A review of the ecological effects of radiofrequency electromagnetic fields (RF-EMF)," *Environ. Int.* **51**, 116–140 (2013).
8. O. Genc, M. Bayrak, and E. Yaldiz, "Analysis of the effects of GSM bands to the electromagnetic pollution in the RF spectrum," *Progr. Electromag. Res.* **101**, 17–32 (2010).
9. N. I. Landy et al., "Perfect metamaterial absorber," *Phys. Rev. Lett.* **100**(20), 207402 (2008).
10. L. Huang and H. T. Chen, "A brief review on terahertz metamaterial perfect absorbers," *Terahertz Sci. Technol.* **6**(1), 26–39 (2013).
11. B. X. Wang and G. Z. Wang, "Quad-band terahertz absorber based on a simple design of metamaterial resonator," *IEEE Photonics J.* **8**(6), 1–8 (2016).
12. W. Xin et al., "Design and characterization of an ultrabroadband metamaterial microwave absorber," *IEEE Photonics J.* **9**(3), 1–13 (2017).
13. K. Yu, Y. Li, and Y. Wang, "A dual-band metamaterial absorber with polarization insensitive and tunable characteristics," in *Int. Applied Computational Electromagnetics Society Symposium-Italy (ACES)*, pp. 1–2, IEEE (2017).
14. G. Sen et al., "A dual band metamaterial inspired absorber for WLAN/Wi-MAX applications using a novel I-shaped unit cell structure," in *Asia-Pacific Microwave Conf. (APMC 2016)*, pp. 1–3, IEEE (2016).

15. N. Thi Quynh Hoa, P. Huu Lam, and P. Duy Tung, "Wide-angle and polarization-independent broadband microwave metamaterial absorber," *Microwave Opt. Technol. Lett.* **59**(5), 1157–1161 (2017).
16. M. Bakir et al., "Tunable perfect metamaterial absorber and sensor applications," *J. Mater. Sci.* **27**(11), 12091–12099 (2016).
17. M. Bağmanç et al., "Broad-band polarization-independent metamaterial absorber for solar energy harvesting applications," *Phys. E* **90**, 1–6 (2017).
18. F. Dincer et al., "Multi-band metamaterial absorber: design, experiment and physical interpretation," *Appl. Comput. Electromag. Soc. J.* **29**(3) (2014).
19. M. Karaaslan et al., "Microwave energy harvesting based on metamaterial absorbers with multi-layered square split rings for wireless communications," *Opt. Commun.* **392**, 31–38 (2017).
20. M. Bakir et al., "Perfect metamaterial absorber-based energy harvesting and sensor applications in the industrial, scientific, and medical band," *Opt. Eng.* **54**(9), 097102 (2015).
21. T. S. Almoneef and O. M. Ramahi, "Metamaterial electromagnetic energy harvester with near unity efficiency," *Appl. Phys. Lett.* **106**(15), 153902 (2015).
22. A. Z. Ashoor and O. M. Ramahi, "Dielectric resonator antenna arrays for microwave energy harvesting and far-field wireless power transfer," *Progr. Electromagnet. Res. C* **59**, 89–99 (2015).
23. S. Heydari Nasab et al., "Investigation of RF signal energy harvesting," *Active Passive Electron. Components* **2010**, 591640 (2010).
24. M. Pinuela, P. D. Mitcheson, and S. Lucyszyn, "Ambient RF energy harvesting in urban and semi-urban environments," *IEEE Trans. Microwave Theory Techn.* **61**(7), 2715–2726 (2013).
25. A. M. Hawkes, A. R. Katko, and S. A. Cummer, "A microwave metamaterial with integrated power harvesting functionality," *Appl. Phys. Lett.* **103**(16), 163901 (2013).
26. H. Gao et al., "A design of 2.4 GHz rectifier in 65 nm CMOS with 31% efficiency," in *2013 IEEE 20th Symp. on Communications and Vehicular Technology in the Benelux (SCVT)*, pp. 1–4, IEEE (2013).
27. D. Wang and R. Negra, "Design of a rectifier for 2.45 GHz wireless power transmission," in *8th Conf. on Ph. D. Research in Microelectronics and Electronics (PRIME)*, pp. 1–4, VDE (2012).
28. B. R. Franciscatto et al., "High-efficiency rectifier circuit at 2.45 GHz for low-input-power RF energy harvesting," in *European Microwave Conf. (EuMC 2013)*, pp. 507–510, IEEE (2013).
29. F. Erkmen, T. S. Almoneef, and O. M. Ramahi, "Electromagnetic energy harvesting using full-wave rectification," *IEEE Trans. Microwave Theory Techn.* **65**(5), 1843–1851 (2017).
30. H. Sun et al., "Design of a high-efficiency 2.45-GHz rectenna for low-input-power energy harvesting," *IEEE Antennas Wireless Propag. Lett.* **11**, 929–932 (2012).
31. G. A. Vera et al., "Design of a 2.45 GHz rectenna for electromagnetic (EM) energy scavenging," in *Radio and Wireless Symp. (RWS 2010)*, pp. 61–64, IEEE (2010).
32. Y. Ushijima et al., "5.8-GHz integrated differential rectenna unit using both-sided MIC technology with design flexibility," *IEEE Trans. Antennas Propag.* **61**(6), 3357–3360 (2013).
33. T. Matsunaga, E. Nishiyama, and I. Toyoda, "5.8-GHz stacked differential rectenna suitable for large-scale rectenna arrays with DC connection," *IEEE Trans. Antennas Propag.* **63**(12), 5944–5949 (2015).
34. Y. S. Chen and C. W. Chiu, "Maximum achievable power conversion efficiency obtained through an optimized rectenna structure for RF energy harvesting," *IEEE Trans. Antennas Propag.* **65**(5), 2305–2317 (2017).
35. Z. Kang et al., "2.45-GHz wideband harmonic rejection rectenna for wireless power transfer," *Int. J. Microwave Wireless Technol.* **9**(5), 977–983 (2017).
36. Y. Xie et al., "A subwavelength resolution microwave/6.3 GHz camera based on a metamaterial absorber," *Sci. Rep.* **7**, 40490(2017).
37. M. T. Ghasr et al., "Portable real-time microwave camera at 24 GHz," *IEEE Trans. Antennas Propag.* **60**(2), 1114–1125 (2012).
38. M. T. Ghasr et al., "Wideband microwave camera for real-time 3-D imaging," *IEEE Trans. Antennas Propag.* **65**(1), 258–268 (2017).
39. O. Altintas et al., "Design of a wide band metasurface as a linear to circular polarization converter," *Modern Phys. Lett. B* **31**(30), 1750274 (2017).
40. L. Man&Tel Co., "Wave and antenna training system," <http://www.scitech.com.my/mats1000.php>.

Cumali Sabah received his BSc, MSc, and PhD degrees in electrical and electronics engineering. Currently, he is an associate professor in the Electrical and Electronics Engineering Department at Middle East Technical University—Northern Cyprus Campus, where he is a secretary general and advisor to the president. His research interests include the microwave and electromagnetic investigation of unconventional materials and structures, wave propagation, scattering, complex media, metamaterials and their applications, and solar systems.

Biographies for the other authors are not available.